

## Antiferromagnetic patches and hidden order in URu<sub>2</sub>Si<sub>2</sub> by impurity doping

S.-H. Baek,<sup>1</sup> M. J. Graf,<sup>1</sup> A. V. Balatsky,<sup>1</sup> E. D. Bauer,<sup>1</sup> J. C. Cooley,<sup>1</sup> J. L. Smith,<sup>1</sup> and N. J. Curro<sup>2</sup><sup>1</sup>Los Alamos National Laboratory, Los Alamos, New Mexico 87545, USA<sup>2</sup>Department of Physics, University of California, Davis, California 95616, USA

(Received 7 October 2009; revised manuscript received 10 February 2010; published 26 April 2010)

We report the use of impurities to probe the hidden order parameter of the strongly correlated metal URu<sub>2</sub>Si<sub>2</sub> below the transition temperature  $T_0 \sim 17.5$  K. The nature of this order parameter has eluded researchers for more than two decades but is accompanied by the development of a partial gap in the single-particle density of states that can be detected through measurements of the electronic specific heat and nuclear-spin-lattice relaxation rate. We find that impurities in the hidden order phase give rise to local patches of antiferromagnetism. An analysis of the coupling between the antiferromagnetism and the hidden order reveals that the former is not a competing order parameter but rather a parasitic effect of the latter.

DOI: 10.1103/PhysRevB.81.132404

PACS number(s): 76.60.-k, 75.30.Kz, 71.27.+a, 74.62.Dh

The heavy fermion URu<sub>2</sub>Si<sub>2</sub> has received considerable attention because it undergoes a phase transition to a state which is poorly understood. The strong interactions between the U *5f* electrons and the delocalized conduction electrons give rise to an enhanced Sommerfeld coefficient  $\gamma = 180$  mJ/mol K<sup>-2</sup> and two phase transitions at low temperature: the hidden order (HO) transition at  $T_0 \sim 17.5$  K gaps approximately 70% of the Fermi-surface area and a superconducting transition at  $T_c \sim 1.4$  K emerges from the remaining charge carriers.<sup>1,2</sup> The large entropy associated with the HO phase transition is suggestive of spin-density wave order, yet direct spin probes have shown no evidence of intrinsic magnetic order in pure crystals. Although the HO phase of URu<sub>2</sub>Si<sub>2</sub> is not itself magnetic, this phase is closely related to antiferromagnetism (AF) of the U electron spins. Early neutron-scattering and muon spin rotation ( $\mu$ SR) studies reported a tiny ordered magnetic moment of  $0.03\mu_B/\text{U}$  in pure URu<sub>2</sub>Si<sub>2</sub>, which led to the concept of small moment antiferromagnetism.<sup>3,4</sup> However, later  $\mu$ SR and nuclear-magnetic-resonance (NMR) measurements tell a quite different story.<sup>2,5</sup> They reveal an inhomogeneous coexistence between small regions of antiferromagnetic order and hidden order in pure URu<sub>2</sub>Si<sub>2</sub>, with a relative fraction that tends toward bulk AF under pressure.<sup>2,3,5</sup> Substituting Rh for Ru in URu<sub>2</sub>Si<sub>2</sub> leads to a suppression of the long-range hidden order and recent neutron-scattering studies revealed large moment AF coexisting with the hidden order for large Rh concentrations.<sup>6</sup>

In order to investigate the microscopic effects of the Rh dopants on the HO phase and to characterize the emergent AF order in U(Ru<sub>1-x</sub>Rh<sub>x</sub>)<sub>2</sub>Si<sub>2</sub>, we have measured the <sup>29</sup>Si NMR spectrum as a function of temperature and Rh concentration. Figure 1 shows a series of such spectra. The resonance frequency of the <sup>29</sup>Si (nuclear spin  $I = \frac{1}{2}$ ) is given by  $f = \gamma H_0(1 + K)$ , where  $\gamma$  is the gyromagnetic ratio of the <sup>29</sup>Si,  $H_0$  is the applied external field (7.42 T), and  $K$  is the Knight shift arising from the hyperfine coupling between the nuclear and electron spins in the solid. Aside from a slight suppression of  $K$  connected with the opening of the gap, we observe no visible change in the spectrum at the HO transition,  $T_0$ , in agreement with previous studies.<sup>7</sup> At lower temperatures we find that two satellite peaks emerge on either side of the

central resonance below a temperature which we define as  $T_N$ , shown in Figs. 1 and 2. These satellites arise because of the presence of a static internal hyperfine field,  $H_{\text{hf}}$ , associated with commensurate AF order with moments pointing along (001), assuming the hyperfine field interaction is isotropic. The nuclei resonate in the local field  $\mathbf{H}_0 + \mathbf{H}_{\text{hf}}$ , where  $H_{\text{hf}} = A\mu_0$ ,  $\mu_0$  is the ordered U spin moment and  $A$  is the hyperfine coupling. We find that  $A$  is unchanged from the pure compound ( $3.6$  kOe/ $\mu_B$ ) (Ref. 7) and can therefore directly measure the AF order parameter,  $M(T, x) \sim \mu_0(T, x)$ , shown in Fig. 2.

The spectra in Fig. 1 reveal an *inhomogeneous* mixture of antiferromagnetic (satellite peaks) and hidden order (central peak) regions below  $T_N$ , characteristic of phase separation. We see no zero-field specific-heat anomaly or critical slowing of  $T_2^{-1}$  at 7.42 T around  $T_N$ , suggesting that this transition is not a new thermodynamic phase but rather a crossover to an inhomogeneous coexistence.<sup>8</sup> The volume fraction of AF domains, shown in Fig. 3, varies with both temperature and doping. The AF fraction saturates at low temperature at a maximum of roughly 70% at  $x = 0.025$ . These observations

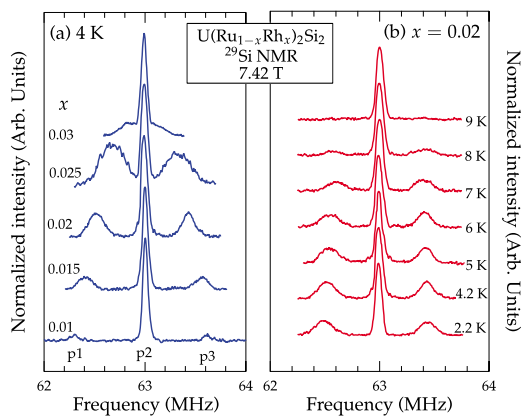


FIG. 1. (Color online) <sup>29</sup>Si spectra in U(Ru<sub>1-x</sub>Rh<sub>x</sub>)<sub>2</sub>Si<sub>2</sub> as a function of  $x$ , panel (a), and temperature  $T$ , panel (b). The spectra were obtained by summing the Fourier transforms of Hahn echoes over several frequencies in a fixed external field along the  $c$  direction. They were normalized to the height of the central peak at each doping or temperature value.

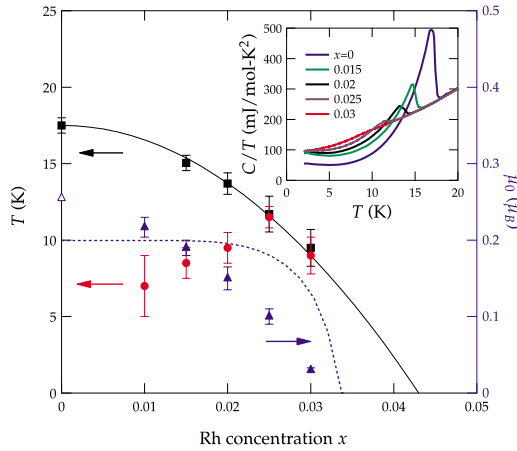


FIG. 2. (Color online) Transition temperature  $T_0$  (at  $H_0=0$  T, black square; left axis),  $T_N$  (at  $H_0=7.42$  T, red circle; left axis) and moment  $\mu_0$  (at  $H_0=7.42$  T, blue triangles; right axis) in  $U(\text{Ru}_{1-x}\text{Rh}_x)_2\text{Si}_2$ . The open triangle at  $x=0$  corresponds to the value of the ordered moment that emerges under pressure in nominally pure  $\text{URu}_2\text{Si}_2$  (Ref. 2).  $T_0$  was determined by the specific-heat anomaly while  $T_N$  was determined by the appearance of the AF peaks as seen in the spectra (Fig. 1) and the AF fraction (Fig. 3). The lines are the calculated  $T_0(x)$  (solid black) and  $\mu_0(x)$  (dashed blue) using the Ginzburg-Landau model described in the text and are renormalized by the critical concentration  $x_c$  (Ref. 9). Inset: specific heat over temperature,  $C/T$ , in zero field vs  $T$  and for different  $x$ . There is no sign of a bulk phase transition at  $T_N$ .

suggest that the AF domains nucleate around the Rh dopants, forming patches with a radius  $\xi_{\text{AF}}$  on the order of two to three lattice spacings at zero temperature. The satellites in the spectrum arise from nuclei within these patches of AF order, whereas the central resonance arises from nuclei outside. The percolation limit is reached at  $x=x_c$ , where the AF patches overlap.

*A priori* these results imply that the AF order characterized by the order parameter  $\mathbf{M}$ , competes with the hidden order, characterized by an order parameter  $\Psi$ . Much like in the vortex cores of the cuprates, a competing AF order parameter can emerge in spatial regions, where the dominant superconducting order parameter is suppressed locally.<sup>10,11</sup> Microscopically the impurities can create local strains that may stabilize  $\mathbf{M}$  in the vicinity of the Rh.<sup>12</sup> However, if this were the case, then  $\mu_0(0,x)$  should increase with doping and long-range AF order would develop above the percolation threshold at  $x_c$ .<sup>13</sup> For example, a competing order parameter is stabilized in Cd doped  $\text{CeCoIn}_5$ , where AF droplets are nucleated at Cd dopants and long-range order develops when they overlap.<sup>14</sup> However, in  $U(\text{Ru}_{1-x}\text{Rh}_x)_2\text{Si}_2$  detailed measurements of the specific heat in zero field as a function of both temperature and doping (see inset of Fig. 2) show no evidence of a second phase transition associated with long-range AF order, either within the HO phase or outside the phase when  $T_0=0$ . Furthermore, as seen in Figs. 1 and 2, the AF order parameter,  $\mathbf{M}(0,x) \sim \mu_0(x)\hat{z}$ , vanishes before  $\Psi(0,x)$  does. In fact, we find that  $\mathbf{M}(0,x)$  scales approximately with  $T_0(x)$  (Fig. 2), suggesting that the AF order is *controlled* by the hidden order and never exists on its own as true long-range order but rather as a parasitic effect within

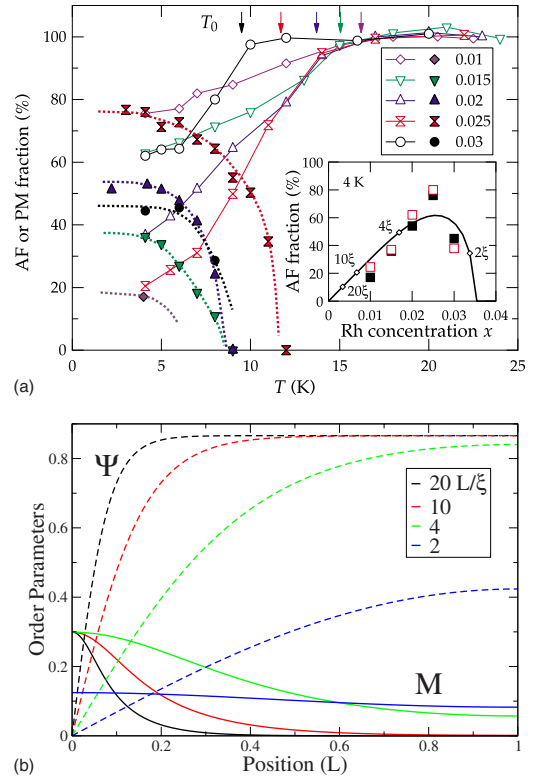


FIG. 3. (Color online) Panel (a): the spectral weight of the AF (filled symbols) and paramagnetic (PM) (open symbols) signals vs  $T$  for different dopings at field 7.42 T. The PM volume fractions are defined as the relative intensities (areas) of the central lines in Fig. 1. Intensities were corrected for the Boltzmann factor and normalized to the high- $T$  values. The AF fractions are relative to the areas of the central PM peaks in the spectra, respectively. Inset: the non-monotonic behavior of the AF fraction versus doping at 4 K. Filled squares are the measured AF fractions while empty squares are the indirect results of the lost fractions of the PM peaks. The solid line is the calculated fraction, equal to the AF magnetization density normalized by the maximum value of  $M$ . Panel (b): within GL theory calculated (Ref. 9) HO order parameter  $\Psi$  (dashed) and AF order parameter  $M$  (solid) vs distance from the Rh impurity for system sizes  $L/\xi=20, 10, 4, 2$  at temperature  $T=T_0/4$ . The corresponding AF fractions are marked by open diamonds in the inset of panel (a).

the HO phase. It is possible that there are in fact two competing effects with Rh doping: (i) local strains that stabilize  $\mathbf{M}$  and (ii) modifications to the electronic structure from the excess carriers introduced by Rh that destabilize both  $\mathbf{M}$  and  $\Psi$  simultaneously. In the latter case, there is no reason for  $\mathbf{M}(x)$  and  $\Psi(0,x)$  to have the same behavior and the simultaneous disappearance of both order parameters implies an unlikely coincidence, which we discard.

Recently, Elgazzar<sup>15</sup> suggested that the HO is a dynamic phenomenon where the Fermi surface is partially gapped to a commensurate AF state that becomes static under pressure. Hence Rh dopants may serve to pin the local fluctuations of  $M_z$ , giving rise to local static patches. However, it is not clear why  $M(x)$  should track  $T_0(x)$  and the HO is completely suppressed when the local patches overlap. It is possible that the Rh doping simultaneously pins the fluctuations and destabi-

lizes the HO via modifications of the electronic structure. As argued above, though, this scenario requires an unlikely coincidence. It also is unclear why the pinning would take place only within a few lattice spacings of the dopant even though the HO is a long-range phenomenon. Finally, we note that there is little difference in the temperature dependence of the spin-lattice relaxation rate measured in the regions of the bulk (central peak) versus the AF droplets (satellites), suggesting the absence of either a dynamic phenomenon or competing order parameter.

In fact, the observed correlation between the AF ordered moment and the HO gap suggest that the AF patches are an epiphenomenon that is a direct consequence of the local suppression of the hidden order in the vicinity of the dopants. We propose that the AF order is coupled to the spatial derivatives of  $\Psi(\mathbf{r})$ . To interpret the results we use the Ginzburg-Landau (GL) (Ref. 16) free-energy functional of the combined system that can be written as  $F[\Psi, \mathbf{M}] = F_{\text{HO}} + F_{\text{AF}} + F_C$ , with  $F_{\text{HO}}[\Psi] = a_1(T - T_0)\Psi^2 + \frac{1}{2}b_1\Psi^4 + \kappa_1|\nabla\Psi|^2 + V\delta(\mathbf{r})\Psi^2$ ,  $F_{\text{AF}}[\mathbf{M}] = a_2|\mathbf{M}|^2 + \frac{1}{2}b_2|\mathbf{M}|^4 + \kappa_2[(\nabla M_x)^2 + (\nabla M_y)^2 + (\nabla M_z)^2]$ , with GL coefficients  $a_1, a_2, b_1, b_2 > 0$ , and impurity potential  $V$ .<sup>9</sup> The coupling term is  $F_C[\Psi, \mathbf{M}] = g_1\Psi^2|\mathbf{M}|^2 + g_2|\mathbf{M}|^2|\nabla\Psi|^2 + g_3|\mathbf{M} \cdot \nabla\Psi|^2$ . The consequences of the first coupling term  $g_1$  have been discussed before<sup>17</sup> while terms  $g_2$  and  $g_3$  give rise to nucleation of inhomogeneous AF order around the impurity site, where the hidden order is suppressed, see Fig. 3(b). A large potential  $V$  leads to the suppression of  $\Psi$  at the impurity site. Since there is no experimental evidence for long-range AF order in the undoped system at zero pressure ( $a_2, g_1 \geq 0$  as well as  $b_1, b_2 > 0$ ), the only way to stabilize a local solution of  $\mathbf{M}(\mathbf{r})$  around an impurity is by demanding that  $g_2, g_3 < 0$ . We can make significant progress by studying a one-dimensional toy model. This will lead to qualitative results only but elucidate the underlying physics. Therefore, we consider only the coupling term  $g_3$  and choose  $\mathbf{M} = (0, 0, M)$  along the applied magnetic field. The effect produced by a  $g_2$  term would be similar to that of  $g_3$  and will be neglected. *From our analysis it follows that if the hidden order is locally suppressed at the Rh dopants, then AF order naturally emerges in regions near Rh atoms, see Fig. 3(b).* The length scale for the recovery of the hidden order, the coherence length  $\xi(T)$ , will then determine the spatial extent of the AF patches and the percolation threshold then corresponds to a suppression of the long-range hidden order. As the hidden order  $\Psi$  is gradually suppressed by Rh dopants the transition temperature  $T_0$  diminishes, as does the induced (or parasitic) AF order  $M$ . If we treat  $M$  as small perturbation to  $\Psi$ , because it vanishes in the bulk, then we can derive an analytic expression for the maximum value  $M_0$  at the impurity site. It agrees qualitatively with the numerical solution and decreases according to  $M_0(T)^2 \sim [2^{-1}|g_3|\xi(T)^{-2}\Psi_0(T)^2 - 2a_2]/b_2$ , where the uniform solution of the unperturbed hidden order is  $\Psi_0(T)^2 = -a_1(T)/b_1$ . This explains why the AF order vanishes before the hidden order with increased doping, a trend that is clearly visible in the data in Figs. 2 and 3, where the AF fraction first increases for small  $x$  and then decreases sharply as AF domains overlap and  $M_0$  is reduced. This observation is consistent with neutron-scattering data seeing no magnetic order outside the HO phase.<sup>6</sup>

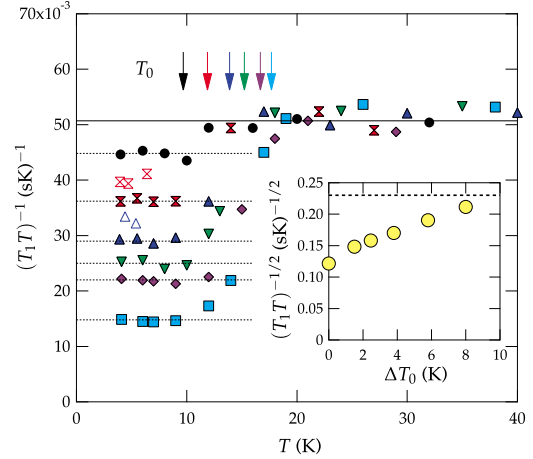


FIG. 4. (Color online)  $(T_1T)^{-1}$  vs  $T$  for doping concentration  $x$ . Same notation as in Fig. 3(a), except for  $x=0$  (cyan square) and  $x=0.03$  (black circle). Solid (open) symbols correspond to the PM central peaks (AF satellites). The solid and dotted lines are guides to the eye. The colored arrows indicate  $T_0(x)$  determined by specific heat. Inset:  $(T_1T)^{-1/2}$  at  $T=4$  K versus  $\Delta T_0 = T_0^0 - T_0$ , where  $T_0^0$  is the bare transition temperature, revealing the increase in  $N(0)$  as the HO gap is filled by impurity states. The dotted line indicates the value of  $(T_1T)^{-1/2}$  above  $T_0$ .

In order to characterize the low-energy density of states (DOS) associated with these localized states near the Rh impurities, we have measured the nuclear-spin-lattice relaxation rate,  $T_1^{-1}$ , as a function of temperature and doping both within and outside of the AF patches. As seen in Fig. 4,  $(T_1T)^{-1} \sim N(0)^2$  is suppressed below  $T_0$  because of the development of the partial gap in the DOS  $N(0)$  at the Fermi surface. With increasing doping,  $(T_1T)^{-1}$  increases monotonically within the HO phase. This behavior is similar to the effect of impurities in unconventional superconductors, suggesting that the Rh impurities induce extra states at low energies.<sup>18,19</sup> In this case, we expect  $(T_1T)^{-1}(x) \sim N^2(0, x) \sim (\Delta T_0)^2(x)$ , consistent with our observations (inset, Fig. 4). Indeed,  $(T_1T)^{-1}$  is faster at the AF satellites in the spectrum (as is the spin-spin relaxation time  $T_2^{-1}$ ), suggesting an excess local DOS within the droplets.

In the case of  $\text{URu}_2\text{Si}_2$  there are multiple bands and one anticipates two distinct scenarios for the gap to fill up. The first corresponds to a gap in the low-energy states for all bands in which case the impurity doping would fill up the DOS for all the bands. A second possibility is that some of the states remain gapless below  $T_0$  while others develop a full gap. In this case, the impurity induces intragap states in the HO gap and essentially does not affect the DOS of the ungapped states. We speculate the latter to be realized for  $\text{URu}_2\text{Si}_2$ . This behavior is also consistent with a subsequent superconducting transition observed at lower temperatures. To test this scenario one needs to observe the DOS in  $\text{URu}_2\text{Si}_2$  as a function of Rh doping in tunneling experiments, such as scanning tunneling or point-contact spectroscopy.

By locally probing the hidden order state of  $\text{U}(\text{Ru}_{1-x}\text{Rh}_x)_2\text{Si}_2$  with NMR in the presence of Rh dopants we have been able to demonstrate that antiferromagnetic or-

der emerges locally near the impurity sites. The induced antiferromagnetic order is an epiphenomenon and depends on the strength of the dominant hidden order. We proposed a minimal Ginzburg-Landau functional of coupled hidden and antiferromagnetic order and found that the induced antiferromagnetic order  $M$  will vanish before the dominant hidden order.

The fact that the AF is manifest only through the spatial gradients of the hidden order rules out theories of orbital AF and helicity order.<sup>20,21</sup> Rather, the hidden order appears to involve compensated spin polarizations on multiple sites such as the triple-spin correlator scenario or an unconventional multiband spin-density wave.<sup>22,23</sup> Similar effects are well known in the study of the NMR hyperfine field at the oxygen sites in the doped high-temperature superconducting cuprates: Zn or Ni impurities substituted at the Cu sites locally perturb the staggered AF order of the Cu  $3d$  spins, giving rise to finite hyperfine fields at the O sites.<sup>24</sup> In the absence of impurities, the hyperfine field at the O site vanishes by symmetry. In  $U(\text{Ru}_{1-x}\text{Rh}_x)_2\text{Si}_2$ , gradients of the HO parameter may lead to noncancellation of the net spin per U site, giving rise to the static  $M_z$  that we observe. Our results

are consistent with induced magnetism  $M$  being *commensurate* with the lattice while the hidden order  $\Psi$  is very likely *incommensurate*, as was argued by Wiebe *et al.*<sup>25</sup> We point out that this discussion implies that Rh doping induces the conversion of HO to a commensurate AF state within each droplet. If indeed the HO state represents an incommensurate charge-density wave (CDW), as argued in Ref. 23, then one would expect that impurities induce spin-dependent scattering that converts CDW order into magnetic excitations and in addition modifies the momentum of the density wave to make it commensurate. Thus it remains a fascinating theoretical and experimental puzzles to explain the sudden conversion of incommensurate hidden order into commensurate antiferromagnetic order in the presence of disorder and possibly pressure.

We thank J. D. Thompson, J. A. Mydosh, P. Oppeneer, P. Coleman, and J. C Davis for stimulating discussions. Work at Los Alamos National Laboratory was performed under the auspices of the U.S. DOE under Contract No. DE-AC52-06NA25396.

<sup>1</sup>T. T. M. Palstra, A. A. Menovsky, J. van den Berg, A. J. Dirkmaat, P. H. Kes, G. J. Nieuwenhuys, and J. A. Mydosh, *Phys. Rev. Lett.* **55**, 2727 (1985).

<sup>2</sup>K. Matsuda, Y. Kohori, T. Kohara, K. Kuwahara, and H. Amitsuka, *Phys. Rev. Lett.* **87**, 087203 (2001).

<sup>3</sup>C. Broholm, J. K. Kjems, W. J. L. Buyers, P. Matthews, T. T. M. Palstra, A. A. Menovsky, and J. A. Mydosh, *Phys. Rev. Lett.* **58**, 1467 (1987).

<sup>4</sup>D. E. MacLaughlin, D. W. Cooke, R. H. Heffner, R. L. Hutson, M. W. McElfresh, M. E. Schillaci, H. D. Rempp, J. L. Smith, J. O. Willis, E. Zirngiebl, C. Boekema, R. L. Lichti, and J. Oostens, *Phys. Rev. B* **37**, 3153 (1988).

<sup>5</sup>G. M. Luke, A. Keren, L. P. Le, Y. J. Uemura, W. D. Wu, D. Bonn, L. Taillefer, J. D. Garrett, and Y. Ōnuki, *Hyperfine Interact.* **85**, 397 (1994).

<sup>6</sup>M. Yokoyama, H. Amitsuka, S. Itoh, I. Kawasaki, K. Tenya, and H. Yoshizawa, *J. Phys. Soc. Jpn.* **73**, 545 (2004).

<sup>7</sup>Y. Kohori, K. Matsuda, and T. Kohara, *J. Phys. Soc. Jpn.* **65**, 1083 (1996).

<sup>8</sup>A. Villaume, F. Bourdarot, E. Hassinger, S. Raymond, V. Taufour, D. Aoki, and J. Flouquet, *Phys. Rev. B* **78**, 012504 (2008).

<sup>9</sup>In our calculations, we used GL parameters  $a_1=b_1=b_2=\kappa_1=1$  and  $a_2=0.02$ ,  $\kappa_2=0.05$ , with coupling coefficients  $g_1=g_2=0$  and  $g_3=-0.5$ .

<sup>10</sup>E. Demler, S. Sachdev, and Y. Zhang, *Phys. Rev. Lett.* **87**, 067202 (2001).

<sup>11</sup>S. A. Kivelson, D.-H. Lee, E. Fradkin, and V. Oganesyan, *Phys. Rev. B* **66**, 144516 (2002).

<sup>12</sup>M. Yokoyama, H. Amitsuka, K. Tenya, K. Watanabe, S. Kawarazaki, H. Yoshizawa, and J. A. Mydosh, *Phys. Rev. B* **72**, 214419 (2005).

<sup>13</sup>Y. Zhang, E. Demler, and S. Sachdev, *Phys. Rev. B* **66**, 094501 (2002).

<sup>14</sup>R. R. Urbano, B. L. Young, N. J. Curro, J. D. Thompson, L. D. Pham, and Z. Fisk, *Phys. Rev. Lett.* **99**, 146402 (2007).

<sup>15</sup>S. Elgazzar, J. Ruzs, M. Amft, P. M. Oppeneer, and J. A. Mydosh, *Nature Mater.* **8**, 337 (2009).

<sup>16</sup>M. Sigrist and K. Ueda, *Rev. Mod. Phys.* **63**, 239 (1991).

<sup>17</sup>N. Shah, P. Chandra, P. Coleman, and J. A. Mydosh, *Phys. Rev. B* **61**, 564 (2000).

<sup>18</sup>A. V. Balatsky, I. Vekhter, and J.-X. Zhu, *Rev. Mod. Phys.* **78**, 373 (2006).

<sup>19</sup>S. Ouazi, J. Bobroff, H. Alloul, M. Le Tacon, N. Blanchard, G. Collin, M. H. Julien, M. Horvatic, and C. Berthier, *Phys. Rev. Lett.* **96**, 127005 (2006).

<sup>20</sup>P. Chandra, P. Coleman, J. A. Mydosh, and V. Tripathi, *Nature (London)* **417**, 831 (2002).

<sup>21</sup>C. M. Varma and L. Zhu, *Phys. Rev. Lett.* **96**, 036405 (2006).

<sup>22</sup>V. Barzykin and L. P. Gor'kov, *Phys. Rev. Lett.* **70**, 2479 (1993).

<sup>23</sup>A. V. Balatsky, A. Chantis, H. P. Dahal, D. Parker, and J. X. Zhu, *Phys. Rev. B* **79**, 214413 (2009).

<sup>24</sup>S. Ouazi, J. Bobroff, H. Alloul, and W. A. MacFarlane, *Phys. Rev. B* **70**, 104515 (2004).

<sup>25</sup>C. R. Wiebe, J. A. Janik, G. J. MacDougall, G. M. Luke, J. D. Garrett, H. D. Zhou, Y.-J. Jo, L. Balicas, Y. Qiu, J. R. D. Copley, Z. Yamani, and W. J. L. Buyers, *Nat. Phys.* **3**, 96 (2007).